6384 *Chem. Mater.* **2010,** *22,* 6384–6392
DOI:10.1021/cm102494j

CHEMISTRY OF MATERIALS
Article

Broadband Nonlinear Absorbing Platinum 2,2′-Bipyridine Complex Bearing 2-(Benzothiazol-2′-yl)-9,9-diethyl-7-ethynylfluorene Ligands

Wenfang Sun,*,† Bingguang Zhang,† Yunjing Li,† Timothy M. Pritchett,‡ Zhongjing Li,† and Joy E. Haley§,∥

†*Department of Chemistry and Biochemistry, North Dakota State University, Fargo, North Dakota 58108-6050, United States,* ‡*U.S. Army Research Laboratory, AMSRD-SE-EM, 2800 Powder Mill Road, Adelphi, Maryland 20783-1197, United States,* §*Materials and Manufacturing Directorate, Air Force Research Laboratory, Wright Patterson Air Force Base, Dayton, Ohio 45433, United States, and* ∥*UES, Inc., Dayton, Ohio 45432, United States*

Received August 31, 2010. Revised Manuscript Received October 25, 2010

A platinum 2,2′-bipyridine complex (**1**) bearing 2-(benzothiazol-2′-yl)-9,9-diethyl-7-ethynylfluorene ligands was synthesized and characterized. Its photophysical properties and nonlinear absorption characteristics were systematically investigated by UV−vis absorption, emission, and transient difference absorption spectroscopy, as well as Z-scan and nonlinear transmission techniques. Complex **1** exhibits a strong structureless $^1\pi,\pi^*$ absorption band at 374 nm and a broad, weak metal-to-ligand charge transfer (^{1}MLCT) transition in the visible region in CH_2Cl_2 solution. It emits at approximately 565 nm with vibronic structures at room temperature in polar solvents, attributed to the acetylide ligand $^3\pi,\pi^*$ excited state. In low-polarity solvents such as hexane and toluene, the emission band becomes structureless and red-shifted, which is assigned to the ^{3}MLCT state. The emission spectrum becomes more structured and slightly blue-shifted at 77 K in butyronitrile glassy matrix. In femtosecond and nanosecond transient absorption measurements, **1** exhibits both singlet and triplet excited-state absorption from 450 to 800 nm, which are tentatively attributed to the $^1\pi,\pi^*/^1$MLCT and $^3\pi,\pi^*/^3$MLCT, respectively. Z scan experiments were carried out using nanosecond and picosecond pulses at 532 nm, and picosecond pulses at a variety of other wavelengths in the visible and near-IR, and the experimental data were fitted by a five-level model using the excited-state lifetimes and estimated cross-section values from the photophysical study. In this way, values were obtained for the first and second singlet excited-state absorption cross sections and the triplet excited-state absorption cross section throughout the visible and near-IR and for the two-photon absorption (TPA) cross section in the near-IR region. Our results demonstrate that **1** possesses extremely large ratios of the excited-state absorption cross sections to the ground-state absorption in the visible spectral region and, compared to the other two-photon absorbing platinum complexes, the largest two-photon absorption cross sections in the near-IR region. This makes complex **1** a very promising candidate for photonic devices that require large and broadband nonlinear absorption. Reverse saturable absorption of **1** in CH_2Cl_2 solution at 532 nm for a nanosecond laser pulse was demonstrated. A remarkable transmission decrease was observed when the incident fluence increased.

Introduction

Platinum diimine complexes containing bis(arylacetylide) ligands have attracted great interest in the past decade due to the ease of structural modification, rich photophysical properties, and versatile potential applications.[1] Eisenberg and co-workers reported the potential application of the platinum diimine triads to a molecular photochemical device based on the photoinduced charge separation in these complexes.[2] Che/Wong and co-workers discovered the use of platinum diimine bisacetylides as potential vapoluminescent materials.[3] Che and co-workers also reported the employment of diimine bis(arylacetylide)platinum(II) complexes in organic light-emitting devices (OLEDs).[4] In addition to these studies, the Eisenberg and Schanze groups independently reported comprehensive structure−property correlation investigations aimed at determining how the substituents on the bipyridine and acetylide ligands influence the excited-state energy and deactivation pathways.[5,6]

*To whom correspondence should be addressed. E-mail: Wenfang.Sun@ndsu.edu. Phone: 701-231-6254. Fax: 701-231-8831.

(1) Williams, J. A. G. *Top. Curr. Chem.* **2007**, *281*, 205.
(2) (a) Hissler, M.; McGarrah, J. E.; Connick, W. B.; Geiger, D. K.; Cummings, S. D.; Eisenberg, R. *Coord. Chem. Rev.* **2000**, *208*, 115. (b) McGarrah, J. E.; Kim, Y.-J.; Hissler, M.; Eisenberg, R. *Inorg. Chem.* **2001**, *40*, 4510.
(3) Lu, W.; Chan, M. C. W.; Zhu, N.; Che, C.-M.; He, Z.; Wong, K. Y. *Chem.—Eur. J.* **2003**, *9*, 6155.
(4) Chan, S.-C.; Chan, M. C. W.; Wang, Y.; Che, C.-M.; Cheung, K.-K.; Zhu, N. *Chem.—Eur. J.* **2001**, *7*, 4180.
(5) (a) Hissler, M.; Connick, W. B.; Geiger, D. K.; McGarrah, J. E.; Lipa, D.; Lachicotte, R. J.; Eisenberg, R. *Inorg. Chem.* **2000**, *39*, 447. (b) Wadas, T. J.; Lachicotte, R. J.; Eisenberg, R. *Inorg. Chem.* **2003**, *42*, 3772.
(6) Whittle, C. E.; Weinstein, J. A.; George, M. W.; Schanze, K. S. *Inorg. Chem.* **2001**, *40*, 4053.

 Published on Web 11/09/2010

Scheme 1

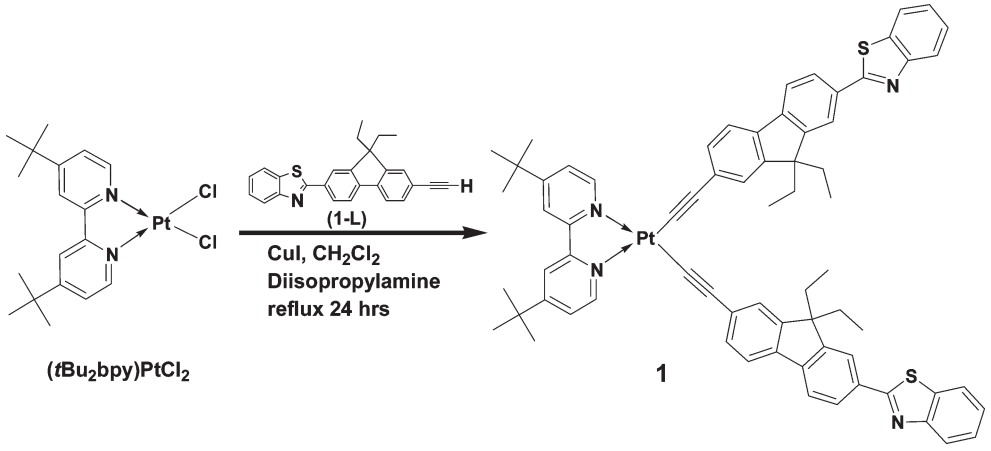

These studies revealed that the energy of the metal-to-ligand charge transfer band (^{1}MLCT) decreases when the electron-withdrawing ability of the substituent on the bipyridine ligand increases or the electron-donating ability of the substituents on the acetylide ligands increases. The photoluminescence energy of these complexes was found to obey the energy gap law when the nature of the substituents on the bipyridine ligand is varied. In contrast, there were no clear trends in the emission energy, lifetimes, and quantum yields when the substituents on the acetylide ligands changed. This was attributed to the interplay of the emitting state between ^{3}MLCT and $^3\pi,\pi$ states. In particular, the emitting state for the complex bearing nitrophenyl acetylide ligands was assigned as a $^3\pi,\pi$ state.[6] The Schanze group further investigated the photophysics and photochemistry of stilbene-containing platinum acetylide complexes and found that the emissive excited state in all of the complexes studied was a $^3\pi,\pi$ state localized on one of the 4-ethynylstilbene ligands.[7] Castellano and co-workers confirmed the interplay between the ^{3}MLCT and $^3\pi,\pi$ states through their study on platinum diimine complexes bearing more conjugated aromatic rings such as 1-pyrene, 1-anthracene, and 1-perylene.[8] Later they reported that the ^{3}MLCT and $^3\pi,\pi$ states could be switched by variation of solvent polarity.[9]

The reported work on the diimine platinum(II) bisacetylides complexes is quite intriguing. However, very little attention has been paid to the nonlinear optical application of the excited-state absorption of these complexes. In view of the broadband triplet excited-state absorption of several reported platinum diimine complexes,[6,7,9] it is expected that these complexes could exhibit reverse saturable absorption in the visible spectral region. To demonstrate this, we recently synthesized a (diimine)platinum(II) complex bearing 2-(benzothiazol-2′-yl)-9,9-diethyl-7-ethynylfluorene ligands (**1**, structure shown in Scheme 1) and studied its reverse saturable absorption at 532 nm for nanosecond and picosecond laser pulses.[10] We found that this complex exhibited very strong reverse saturable absorption for both nanosecond and picosecond laser pulses at 532 nm, with the ratio of the triplet excited-state absorption to ground-state absorption cross sections (σ_T/σ_G) being as high as 754, the largest value reported to date for σ_T/σ_G at 532 nm.

Our preliminary result on the nonlinear absorption of **1** is very exciting. In order to utilize the excited state absorption, we have to populate the excited state from the ground state upon excitation. Unfortunately, above 600 nm the ground-state absorption of most of the platinum diimine complexes is very weak or nonexistent. This would prevent the population of the excited state via one-photon absorption, which in turn would prevent us from utilizing the excited-state absorption. To solve this problem, we introduced the 2-(benzothiazol-2′-yl)-9,9-diethyl-7-ethynylfluorene ligands on complex **1** because platinum complexes containing this ligand have been reported to exhibit two-photon absorption in the near-IR region.[11] We anticipate that complex **1** will exhibit broadband nonlinear absorption from the visible to the near-IR region via one-photon or two-photon induced excited-state absorption. An added advantage of incorporating the ethynylfluorene ligands is that we could adjust the solubility and intermolecular $\pi-\pi$ stacking of the complex by alternation of the alkyl chains at the 9-position of the fluorene units.

In this work, we report the synthesis of **1**, and our systematical studies on its photophysical and nonlinear absorption properties in the visible and the near-IR regions. The nonlinear absorption of the complex was investigated using the Z scan technique. By fitting the Z-scan results using a five-level model, we obtained values of the singlet and triplet excited-state absorption cross sections and of the two-photon absorption cross section

(7) Haskins-Glusac, K.; Ghiviriga, I.; Abboud, K. A.; Schanze, K. S. *J. Phys. Chem. B* **2004**, *108*, 4969.
(8) (a) Castellano, F. N.; Pomestchenko, I. E.; Shikhova, E.; Hua, F.; Muro, M. L.; Rajapakse, N. *Coord. Chem. Rev.* **2006**, *250*, 1819. (b) Pomestchenko, I. E.; Luman, C. R.; Hissler, M.; Ziessel, R.; Castellano, F. N. *Inorg. Chem.* **2003**, *42*, 1394.
(9) Pomestchenko, I. E.; Castellano, F. N. *J. Phys. Chem. A* **2004**, *108*, 3485.
(10) Pritchett, T. M.; Sun, W.; Zhang, B.; Ferry, M. J.; Li, Y.; Haley, J. E.; Mackie, D.; Shensky, W.; Mott, A. G. *Opt. Lett.* **2010**, *35*, 1305.
(11) Rodgers, J. E.; Slagle, J. E.; Krein, D. M.; Burke, A. R.; Hall, B. C.; Fratini, A.; McLean, D. G.; Fleitz, P. A.; Cooper, T. M.; Drobizhev, M.; Makarov, N. S.; Rebane, A.; Kim, K.-Y.; Farley, R.; Schanze, K. S. *Inorg. Chem.* **2007**, *46*, 6483.

of **1** at various wavelengths in the visible and near-IR. Our results show that complex **1** possesses extremely large ratios of the excited-state absorption cross section to the ground-state absorption in the visible spectral region and the largest two-photon absorption cross section for platinum complexes reported to date in addition to its broadband nonlinear response.

Experimental Section

Materials and Characterization. All of the reagents were purchased from Aldrich Chemical Co. or Alfa Aesar and used as is. The ligands 4,4′-di(*tert*-butyl)-2,2′-bipyridine (tBu$_2$bpy)[12] and 2-(benzothiazol-2′-yl)-9,9-diethyl-7-ethynylfluorene (**1-L**),[11] and the precursor (tBu$_2$bpy)PtCl$_2$[13] were prepared according to the literature procedures. All of the solvents purchased from VWR International are HPLC grade and used without further purification unless otherwise stated. The precursors and complex **1** were characterized by ^{1}H NMR, electrospray ionization mass spectrometry (ESI-MS), and elemental analyses. ^{1}H NMR spectra were obtained on a Varian Oxford-400 VNMR spectrometer or a Varian Oxford-500 VNMR spectrometer. ESI-MS analyses were performed with a Bruker BioTOF III mass spectrometer. Elemental analyses were carried out by NuMega Resonance Laboratories, Inc. in San Diego, California.

Synthesis of Complex 1. The ligand **1-L** (200 mg, 0.53 mmol) and (tBu$_2$bpy)PtCl$_2$ (134 mg, 0.25 mmol) were dissolved in degassed dry CH_2Cl_2 (50 mL) and diisopropyl amine (5 mL). The catalyst CuI (∼5−10 mg) was then added. The reaction mixture was refluxed under argon for 24 h. After cooling to room temperature, the reaction solution was washed with brine and dried with Na_2SO_4 and the solvent was removed. The residual solid was purified by column chromatography on silica gel using CH_2Cl_2 as the eluent. The product was further purified by recrystallization from dichloromethane and hexane to yield yellow needle crystal 0.21 g (yield: 64%). ^{1}H NMR (400 MHz, $CDCl_3$): δ 9.75 (d, 2H, J = 6.0 Hz), 8.08 (s, 2H), 8.06 (d, 2H, J = 8.4 Hz), 8.00 (dd, 2H, J = 8.0 Hz, 1.6 Hz), 7.96 (s, 2H), 7.88 (d, 2H, J = 8.0 Hz), 7.72 (d, 2H, J = 8.0 Hz), 7.64 (d, 2H, J = 8.0 Hz), 7.55−7.63 (m, 6H), 7.46 (dt, 2H, J = 8.0 Hz, 1.2 Hz), 7.34 (dt, 2H, J = 8.0 Hz, 1.2 Hz), 7.26−7.32 (m, 1H), 2.03−2.15 (m, 4H), 1.43 (s, 18H), 0.36 (t, 6H, J = 7.6 Hz). ESI-HRMS: m/z calcd for $[C_{70}H_{64}N_4PtS_2 + H + Na]^+$: 1243.4130; found, 1243.4123. Anal. Calcd for $C_{70}H_{64}N_4PtS_2 \cdot C_6H_{14}$, C, 69.86; H, 6.02; N, 4.29. Found: C, 69.67; H, 6.31; N, 4.57.

Photophysical Measurements. The UV−vis absorption spectra were acquired on an Agilent 8453 spectrophotometer in different HPLC grade solvents. The steady-state emission spectra were recorded on a SPEX fluorolog-3 fluorometer/phosphorometer in different solvents. The emission quantum yields were determined by the relative actinometry method[14] in degassed solutions, in which a degassed aqueous solution of $[Ru(bpy)_3]Cl_2$ (Φ_{em} = 0.042, λ_{ex} = 436 nm)[15] was used as the reference. The femtosecond transient absorption measurements were performed using a femtosecond pump−probe UV−vis spectrometer (HELIOS) manufactured by Ultrafast Systems LLC. The sample solution in a 2 mm cuvette was excited at 400 nm using a 150 fs Ti:Sapphire laser (Spectra Physics Hurricane, 1 kHz repetition rate, 1 mJ/pulse at 800 nm), and the absorption was probed from 425 to 800 nm with sapphire generated white-light continuum. The emission lifetime and the triplet transient difference absorption (TA) spectrum and the decay time were measured in degassed solutions on an Edinburgh LP920 laser flash photolysis spectrometer. The third harmonic output (355 nm) of a Nd:YAG laser (Quantel Brilliant, pulsewidth ∼4.1 ns, repetition rate was set at 1 Hz) was used as the excitation source. Each sample was purged with Ar for 30 min before each measurement.

The triplet excited-state absorption coefficient (ε_T) at the TA band maximum was determined by the singlet depletion method.[16] The following equation was used to calculate the ε_T.[16]

$$\varepsilon_T = \frac{\varepsilon_S[\Delta OD_T]}{\Delta OD_S}$$

where ΔOD_S and ΔOD_T are the optical density changes at the minimum of the bleaching band and the maximum of the positive band in the TA spectrum, and ε_S is the ground-state molar extinction coefficient at the wavelength of the bleaching band minimum. After the ε_T value is obtained, the triplet excited-state quantum yield could be obtained by the relative actinometry,[17] in which SiNc in benzene was used as the reference (ε_{590} = 53 400 M^{-1} cm^{-1}, Φ_T = 0.20).[18]

Z-Scan Measurements and Fittings. The open aperture Z-scan measurements were carried out using a nanosecond laser at 532 nm and picosecond laser from 450 to 900 nm. The experimental setup and experimental details were similar to those reported previously by our group.[19] The experimental data were fitted using a five-level model. The details of the model and fitting procedure were reported previously.[19]

Nonlinear Transmission Measurement. The nonlinear transmission experiment was carried out using 4.1 ns laser pulses at 532 nm. A Quantel Brilliant nanosecond laser with a repetition rate of 10 Hz was used as the light source. The experimental setup and details are the same as previously described.[20] The focal length of the plano-convex lens used to focus the beam to the 2 mm thick sample cuvette was 20 cm.

Results and Discussion

Electronic Absorption. The UV−vis absorption of **1** obeys Lambert−Beer's law in the concentration range used in our study (2×10^{-6} to 1×10^{-4} mol/L), indicating that no ground-state aggregation occurs in this concentration range. Figure 1 displays the UV−vis absorption spectrum of **1** in CH_2Cl_2 solution. The spectrum of **1-L** is presented in the inset for comparison. The molar extinction coefficients are provided in Table 1. The absorption spectrum of **1** is dominated by a broad, structureless band at ∼374 nm, which is red-shifted approximately 20 nm compared to the absorption band of **1-L**. The similarity in the energy of this band to that of the ligand indicates that

(12) (a) Vicente, J.; Gonzalez-Herrero, P.; Perez-Cadenas, M.; Jones, P. G.; Bautista, D. *Inorg. Chem.* **2007**, *46*, 4718. (b) Rendina, L. M.; Vittal, J. J.; Puddephatt, R. J. *Organometallics* **1995**, *14*, 1030.
(13) Adams, C. J.; James, S. L.; Liu, X.; Raithby, P. R.; Yellowlees, L. J. *J. Chem. Soc., Dalton Trans.* **2000**, 63.
(14) Demas, J. N.; Crosby, G. A. *J. Phys. Chem.* **1971**, *75*, 991.
(15) Van Houten, J.; Watts, R. *J. Am. Chem. Soc.* **1976**, *98*, 4853.
(16) Carmichael, I.; Hug, G. L. *J. Phys. Chem. Ref. Data* **1986**, *15*, 1.
(17) Kumar, C. V.; Qin, L.; Das, P. K. *J. Chem. Soc., Faraday Trans.* **1984**, *280*, 783.
(18) Firey, P. A.; Ford, W. E.; Sounik, J. R.; Kenney, M. E.; Rodgers, M. A. J. *J. Am. Chem. Soc.* **1988**, *110*, 7626.
(19) (a) Li, Y.; Pritchett, T. M.; Huang, J.; Ke, M.; Shao, P.; Sun, W. *J. Phys. Chem. A* **2008**, *112*, 7200.(b) Ji, Z.; Li, Y.; Pritchett, T. M.; Makarov, N. S.; Haley, J. E.; Li, Z., Drobizhev, M.; Rebane, R.; Sun, W. Chem.—Eur. J. Accepted for publication.
(20) Sun, W.; Zhu, H.; Barron, P. M. *Chem. Mater.* **2006**, *18*, 2602.

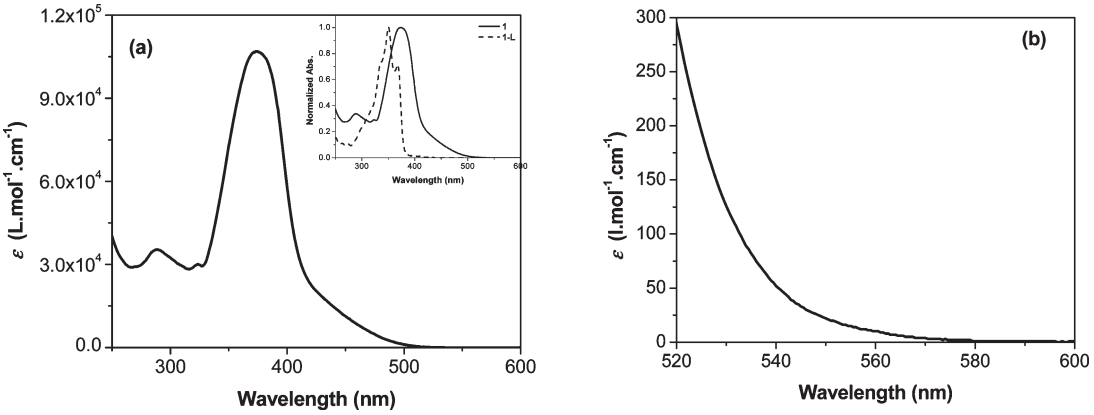

Figure 1. (a) UV−vis absorption spectrum of complex **1** in CH_2Cl_2 solution. The inset shows the normalized UV−vis absorption spectra of **1** and **1-L** in CH_2Cl_2 solution. (b) Expansion of the UV−vis spectrum of **1** between 520 and 600 nm in CH_2Cl_2.

Table 1. Photophysical Parameters of 1

λ_{abs}/nm (log ε/L mol^{-1} cm^{-1})[a]	λ_{em}/nm (Φ_{em}; τ_0/μs; k_Q/L mol^{-1} S^{1-})[b]	λ_{em}/nm (τ/μs)[c]	λ_{S1-Sn}/nm (τ_S/ps)[d]	λ_{T1-Tn}/nm (ε_{T1-Tn}/L mol^{-1} cm^{-1}; τ_{TA}/μs; Φ_T)[e]
288 (4.55), 374 (5.03), 423 (4.33)	565 (0.20; 10.7; 6.22 × 10^8)	552 (289), 604 (273)	606 (145 ± 105)	620 (60170; 10.8; 0.14)

[a] UV−vis absorption band maxima and molar extinction coefficients in CH_2Cl_2. [b] Emission band maximum, quantum yield, intrinsic lifetime, and self-quenching rate constant in CH_2Cl_2. [c] Emission band maxima and lifetimes in BuCN matrix at 77 K. [d] Femtosecond TA band maximum and singlet excited-state lifetime in CH_2Cl_2. [e] Nanosecond TA band maximum, triplet extinction coefficient, triplet excited-state lifetime, and quantum yield in CH_2Cl_2.

it likely arises from the $^1\pi,\pi^*$ transition of the acetylide ligand **1-L**. This assignment is consistent with the minor solvent effect observed for this band, which is similar to that observed in the ligand (Supporting Information, Figure S1). However, the bathochromic shift of this band compared to that of the ligand implies that there should be some delocalization of the ligand-centered molecular orbitals through the interactions with the platinum dπ orbitals. This notion of delocalized molecular orbitals is also supported by the lack of vibronic structure in this band, which is indicative of weak electron-vibronic coupling and is in line with a delocalized excited state. A similar observation was reported by Schanze and co-workers for the stilbene-containing platinum diimine acetylide complex.[7]

In addition to the major band at 374 nm, a low-energy tail is observed between 410 and 500 nm in the spectrum of **1**. This band is red-shifted in less polar solvents, such as hexane and toluene (Supporting Information, Figure S1), indicative of the charge-transfer nature of this band. With reference to that reported for other diimine platinum acetylides complexes, this band can be attributed to the ^{1}MLCT transition.[5−9]

Photoluminescence. Complex **1** is emissive in fluid solutions at room temperature and in butyronitrile matrix at 77 K. Figure 2 shows the normalized emission spectra of **1** in different solvents. The emission spectra are independent of the excitation wavelengths. The same emission spectra were obtained when excited at wavelengths from 380 to 550 nm (Supporting Information, Figure S2). The emission lifetimes and quantum yields are listed in Table 2. The emission in all solvents exhibits a significant Stokes shift, and the lifetimes in most polar solvents are around 10 μs. In addition, the emission is quite sensitive to

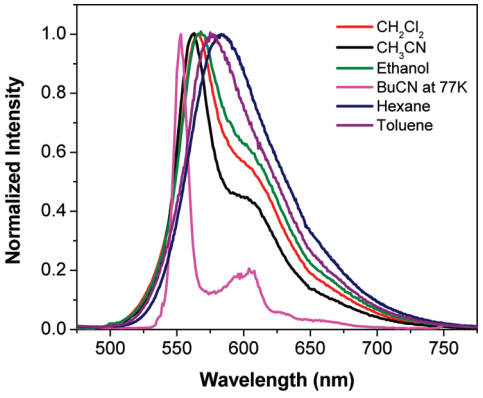

Figure 2. Normalized emission spectra of complex **1** in different solvents at room temperature and in butyronitrile glassy matrix at 77 K.

Table 2. Emission and TA Parameters of Complex 1 in Different Solvents at Room Temperature

solvent	acetone	CH_2Cl_2	CH_3CN	ethanol	hexane[a]	toluene[b]
Φ_{em}	0.10	0.20	0.081	0.085	0.22	0.31
λ_{em}/nm	567	565	562	567	583	576
τ_{em}/ns	8060	10720	7620	9850	900	1400
λ_{T1-Tn}/nm		620	608			622
τ_{T1-Tn}/ns		10780	7870			1320

[a] With 10% 1,2-dichloroethane. [b] With ~4% CH_2Cl_2.

oxygen quenching. Taking all these facts into account and referring to the other reported platinum diimine acetylide complexes,[5−9] the emission from **1** at room temperature should originate from a triplet excited state. However, the nature of the emitting state varies in different solvents. As shown in Figure 2, in polar solvents like CH_3CN, CH_2Cl_2, and ethanol, an apparent vibronic structure is evident, with a vibronic spacing of approximately 1100 cm^{-1},

which corresponds to the ring breathing mode of the aromatic ring. The polarity of the solvent has a minor effect on the feature and energy of the emission in polar solvents. Therefore, the emitting state could be regarded as dominated by the $^3\pi,\pi^*$ state that is primarily localized on the acetylide ligand. This assignment is also supported by the minor solvent quenching in a coordinating solvent such as CH_3CN, in which the emission lifetime is similar to that in noncoordinating solvent like CH_2Cl_2. In contrast, in low-polarity solvents, such as hexane and toluene, the emission band is red-shifted and becomes featureless. The lifetime becomes much shorter compared to those in polar solvents. This suggests that the emitting state in low-polarity solvents is likely a charge transfer state, i.e., the ^{3}MLCT state. The switch of the emitting state from the $^3\pi,\pi^*$ state in polar solvents to the ^{3}MLCT state in low-polarity solvents is attributed to the different solvent-dependency of these two states. The ^{3}MLCT excited state would become more stabilized in low-polarity solvent compared to that in polar solvents, while the $^3\pi,\pi^*$ state is much less affected by the polarity of the solvent. Therefore, the energy of the ^{3}MLCT excited state decreases more than the $^3\pi,\pi^*$ state and becomes the lowest excited state at low-polarity solvents, which results in structureless and relatively short-lived emission. Solvent-induced switching of the emitting state between charge transfer and intraligand excited states has been reported by Castellano and co-workers in platinum diimine complex bearing naphthylacetylide ligands.[9]

The emission of **1** in CH_2Cl_2 at different concentrations was also investigated. The results show that the shape of the emission spectrum remains the same in the concentration range of 2×10^{-6} to 1×10^{-4} mol/L and that the emission intensity increases with increased concentration (Supporting Information, Figure S3). However, the lifetime decreases with increased concentration. This clearly indicates self-quenching. The self-quenching rate constant was measured to be 6.22×10^8 L mol^{-1} s^{-1}, which is in line with the self-quenching rate constant for other platinum diimine complexes reported by Eisenberg[5a] and for many other square-planar platinum complexes reported by our group and several other groups.[21] The intrinsic lifetime for **1** is deduced to be $\sim$10.7 μs.

Complex **1** is also emissive in butyronitrile glassy matrix at 77 K. As shown in Figure 2, the emission spectrum at 77 K is slightly blue-shifted and becomes narrower and more structured, with a vibronic spacing of approximately 1560 cm^{-1}. The thermally induced Stokes shift is approximately 420 cm^{-1}. The lifetime of the emission is 289 μs measured at 552 nm. The small thermally induced Stokes shift, the vibronic structure, and the long lifetime suggest that the emission at 77 K should originate from the $^3\pi,\pi^*$ excited state of the acetylide ligand as well.

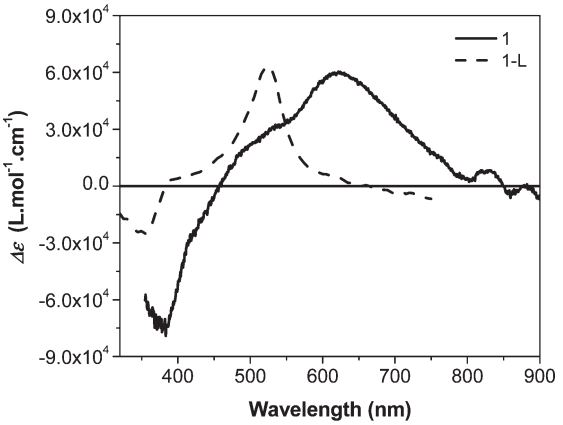

Figure 3. The T_1-T_n transient difference absorption spectra of **1** in CH_2Cl_2 and **1-L** in butyronitrile at zero time delay after the excitation at 355 nm. $c = 4.75 \times 10^{-6}$ mol/L for **1** and 9.76×10^{-6} mol/L for **1-L**.

Transient Absorption. The nanosecond and femtosecond transient difference absorption (TA) spectra of the complex were studied to understand the triplet and singlet excited-state absorption and kinetics. The nanosecond transient difference absorption spectra of complex **1** and the ligand **1-L** in CH_2Cl_2 solution at zero time delay are presented in Figure 3. Both **1** and **1-L** exhibit similar spectral features, with a positive absorption band appearing in the visible spectral region and a bleaching band below 400 nm. However, the spectrum of **1** is red-shifted compared to that of **1-L**. Specifically, the absorption band maximum for **1** appears at 620 nm, while it occurs at 525 nm for **1-L**. The extinction coefficients at the band maximum along with the lifetimes deduced from the decay of the transient absorption for **1** are listed in Table 1. The triplet excited-state quantum yield was determined to be 0.14 for **1** using the relative actinometry. It is noteworthy that the triplet lifetime deduced from the decay of the TA for **1** (10.8 μs) is consistent with that obtained from the decay of the emission. This implies that the excited state that gives rise to the transient absorption is either the same excited state that emits or else is in equilibrium with the emitting state. In view of this fact and the similar features of the TA spectra of **1** and **1-L**, we tentatively attribute the transient absorption to the $^3\pi,\pi^*$ excited state primarily localized on the acetylide ligand. However, the red-shift of the TA spectrum of **1** relative to that of **1-L** suggests that the ligand centered molecular orbitals are somewhat delocalized through interactions with the platinum dπ orbitals. This is similar to what is observed in the UV−vis absorption spectrum for the singlet excited state and is in line with what has been reported for platinum complex containing the similar acetylide ligand.[22] This notion is further supported by the reduced triplet excited-state lifetime of **1** in comparison to that of the acetylide ligand (29.2 μs). On one hand,

(21) (a) Guo, F.; Sun, W.; Liu, Y.; Schanze, K. *Inorg. Chem.* **2005**, *44*, 4055. (b) Shao, P.; Li, Y.; Sun, W. *Organometallics* **2008**, *27*, 2743. (c) Ji., Z.; Li., Y.; Sun, W. *Inorg. Chem.* **2008**, *47*, 7599. (d) Shao, P.; Li, Y.; Azenkeng, A.; Hoffmann, M.; Sun, W. *Inorg. Chem.*. **2009**, *48*, 2407. (e) Shao, P.; Li, Y.; Yi, J.; Pritchett, T. M.; Sun, W. *Inorg. Chem.* **2010**, *49*, 4507. (f) Lai, S.-W.; Chan, M. C.-W.; Cheung T.-C.; Peng, S.-M.; Che, C.-M. *Inorg. Chem.* **1999**, *38*, 4046. (g) Yam, V. W.-W.; Tang, R. P.-L.; Wong, K. M.-C.; Cheung, K.-K. *Organometallics* **2001**, *20*, 4476.

(22) Rogers-Haley, J. E.; Monahan, J. L.; Krein, D. M.; Slagler, J. E.; McLean, D. G.; Cooper, T. M.; Urbas, A. M. *Proc. SPIE* **2008**, *7049*, 704906–1.

this reflects the heavy-atom effect of the platinum that increases the rate of decay from the T_1 to S_0. On the other hand, the reduced energy of the $^3\pi,\pi^*$ excited state also leads to reduced lifetimes according to the energy gap law.[23] Alternatively, the reduced lifetime of **1** relative to **1-L** could imply that the excited state that gives rise to the transient absorption is not a pure $^3\pi,\pi^*$ state but rather a mixed state with some ^{3}MLCT character. This notion could be partially supported by the TA measurement in CH_3CN and toluene, two solvents representing the polar and less polar solvent. As seen in the Supporting Information, Figure S4, the TA spectra in these two solvents are quite similar; however, the spectrum in toluene possesses a more apparent shoulder between 420 and 520 nm. In contrast, the lifetime deduced from the decay of TA is quite distinct in these two solvents. The lifetime in CH_3CN solution is much longer than that in toluene solution, which is consistent with those acquired from the decay of the emission. In view of the much shorter lifetime in toluene compared to that in CH_3CN, we believe that the dominant contributor to the TA in toluene is the ^{3}MLCT state, although the $^3\pi,\pi^*$ manifold likely contributes as well. The composition of the two states in polar solvents should be reversed, with the $^3\pi,\pi^*$ character dominating and possibly mixed with some ^{3}MLCT character. The variation of the different composites in different solvents has previously been suggested by Castellano and co-workers for diimine platinum complex bearing naphthylacetylide ligand.[9]

To understand the singlet excited-state absorption and obtain the lifetime of the singlet excited state, which will be used as an input parameter for fitting the Z-scan data, femtosecond transient absorption measurements were carried out. The time-resolved TA spectrum of **1** in CH_2Cl_2 is given in Figure 4, which is measured using ultrafast femtosecond laser excitation (150 fs) at 400 nm. Immediately following the excitation pulse, the absorption occurs at 606 nm, which is similar to the S_1—S_n absorption band maximum (λ_{max} = 623 nm) of the ligand **1-L** in benzene (Supporting Information, Figure S5). Therefore, the transient absorption of **1** right after the excitation could be tentatively assigned to the acetylide ligand centered $^1\pi,\pi^*$ absorption. However, the somewhat different shapes of the two spectra imply that other excited states, likely the ^{1}MLCT state could also contribute to the spectrum of **1**. At longer delay time, the band maximum bathochromically shifts to 620 nm, accompanied by an isosbestic point at 450 nm. This reflects the intersystem crossing from the $^1\pi,\pi^*/^1$MLCT states to the $^3\pi,\pi^*/^3$MLCT excited states. The spectrum at longer delay time is essentially the same as that measured by nanosecond laser flash photolysis (shown in Figure 3). Therefore, it is also attributed to the mixed $^3\pi,\pi^*/^3$MLCT absorption as we discussed in the previous paragraph for

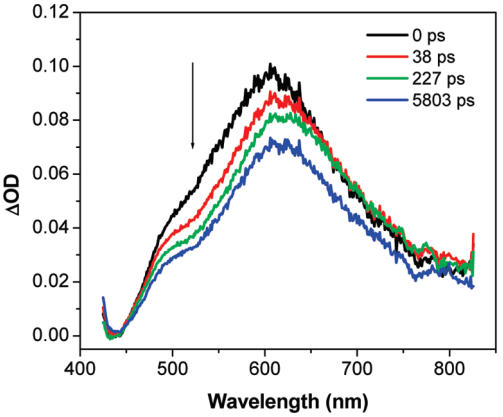

Figure 4. Time-resolved femtosecond transient difference absorption spectrum of **1** in CH_2Cl_2 solution at room temperature. λ_{ex} = 400 nm. $c = 7 \times 10^{-5}$ mol/L.

nanosecond TA. The population of both $^3\pi,\pi^*$ and ^{3}MLCT states via intersystem crossing was reported previously for Ru complexes.[24] The decay of the femtosecond TA spectrum exhibits multiexponential kinetics. The fast decay of 16.0 ± 6.7 ps should be attributed to the internal conversion from the higher singlet excited state, the vibrational relaxation, and the solvent reorganization of the molecule. The lifetime of 145 ± 105 ps is presumably assigned as the decay of the singlet excited state including intersystem crossing and internal conversion. A long lifetime that far exceeds the 6000 ps delay line of our experiment should be due to the decay of the triplet excited state. Although we cannot distinguish the time scale for the intersystem crossing from the $^1\pi,\pi^*$ to $^3\pi,\pi^*$ and that from ^{1}MLCT to ^{3}MLCT using the available data, the singlet lifetime measured is only utilized in the Z-scan data fitting and is mainly of interest for our purposes. The singlet lifetime of **1** is obviously much shorter than that of the acetylide ligand **1-L** (589 ps, measured in CH_2Cl_2), which should be attributed to the rapid intersystem crossing induced by the heavy-atom effect of platinum.

Z Scan. Both the nanosecond and femtosecond transient absorption spectra indicate that complex **1** exhibits relatively strong singlet and triplet excited-state absorption from 450 to 800 nm. However, the observed transient difference absorption is likely a combination of the excited-state absorption from the first excited state to the second excited state ($S_1 \rightarrow S_2$ or $T_1 \rightarrow T_2$) and from S_2 or T_2 to a higher excited state S_n or T_n (S indicates the singlet excited state and T refers to the triplet excited state). It is not possible to deconvolve these contributions using the transient absorption measurement alone. To obtain the absorption cross sections of the singlet and triplet excited states and separate the contributions from S_1 and S_2 states, open-aperture Z scans were carried out at 532 nm using both nanosecond and picosecond laser pulses and at a variety of visible and near-IR wavelengths using picosecond laser pulses having a series of different energies. It is expected that at lower pulse energies only the lowest lying excited states will be populated, and the singlet excited-state absorption would be dominated by

(23) Caspar, J. V.; Meyer, T. J. *J. Phys. Chem.* **1983**, *87*, 952.
(24) (a) Sun, Y.; Joyce, L. E.; Dickson, N. M.; Turro, C. *Chem. Commun.* **2010**, *46*, 2426. (b) Shaw, J. R.; Webb, R. T.; Schmehl, R. H. *J. Am. Chem. Soc.* **1990**, *112*, 1117. (c) Tyson, D. S.; Luman, C. R.; Zhou, X.; Castellano, F. N. *Inorg. Chem.* **2001**, *40*, 4063.

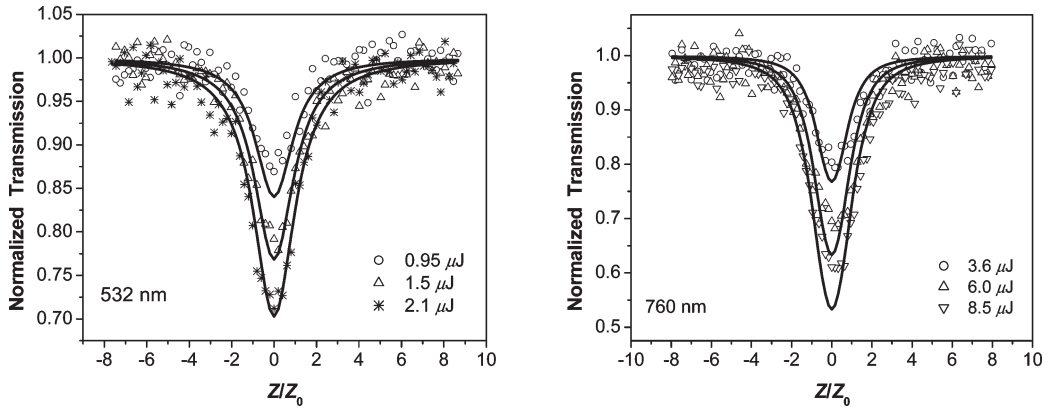

Figure 5. Picosecond Z-scan experimental data (symbols) and fitting curves (solid lines) for **1** in CH_2Cl_2 solution at 532 and 760 nm with different excitation energies. The spot size at the focal plane is 29 μm at 532 nm and 39 μm at 760 nm. The solution concentration is 1.36×10^{-3} mol/L for the 532 nm measurement and 1.28×10^{-2} mol/L for the 760 nm measurement.

Table 3. Absorption Cross Sections of 1 in CH_2Cl_2 Solution[a]

	10^{-18} cm^2							GM
λ (nm)	σ_0[b]	σ_{S1}[c]	σ_T[d]	σ_{S2}[e]	σ_{S1}/σ_0	σ_T/σ_0	σ_{S2}/σ_0	σ_2[f]
450	39.4	35	94[h]	120	0.89	2.4	3.0	
475	21.2	46	250[h]	70	2.2	11.8	3.3	
500	5.55	48	375[h]	70	8.6	67.6	12.6	
532	0.383	60	460	70	157	1.20×10^3	183	
550	0.0765	75	550[h]	70	980	7.19×10^3	915	
575	0.0188	95	760[h]	350	5.05×10^3	4.04×10^4	1.86×10^4	
600	0.0084	110	900[h]	1000	1.31×10^4	1.07×10^5	1.19×10^5	
630	~0	100[g]	870[h]	30				1000
680	~0	70[g]	650[h]	30				400
740	~0	40[g]	400[h]	10				600
760	~0	34[g]	285[h]	10				1000
800	~0	28[g]	320[h]	10				300
825	~0	28[g]	240[h]	1				80
850	~0							600[i]
875	~0							300[i]
900	~0							300[i]

[a] Determined by fitting Z-scan data except where otherwise indicated. [b] The ground-state absorption cross section. [c] The first singlet excited-state absorption cross section. [d] The effective triplet excited-state absorption. [e] The second singlet excited-state absorption cross section. [f] The two-photon absorption cross section. [g] Determined from the value $\sigma_S(532\text{ nm}) = 6 \times 10^{-17}$ cm^2 and the femtosecond transient difference absorption spectrum at 0 time delay. [h] $\sigma_T(532\text{ nm}) = 4.6 \times 10^{-16}$ cm^2 determined from combined fitting of nanosecond and picosecond Z-scan data. For other wavelength, $\sigma_T(\lambda)$ is determined from the value of $\sigma_T(532\text{ nm})$ and the femtosecond transient difference absorption spectrum at 5.8 ns time delay. [i] Effective cross-section for excited-state-assisted two-photon absorption.

the absorption of $S_1 \rightarrow S_2$. At higher excitation energies, however, the S_2 state could acquire a significant population so that the absorption driving the transition $S_2 \rightarrow S_n$ would make a non-negligible contribution to the Z-scan signal, which would have to be taken into account. At longer wavelengths where the ground-state absorption of **1** is negligible, it is still possible to populate the excited state via two-photon absorption (TPA), so at these wavelengths two-photon absorption from the ground state in combination with subsequent excited-state absorption should be considered. To obtain values for the various absorption cross sections, the Z-scan experimental data were fitted by a five-level model that tracks the relative populations of the ground state S_0 and of the S_1, S_2, T_1, and T_m excited states, where T_m denotes a triplet excited state lying above T_1. The various photophysical parameters that appear in the model were determined from independent measurements: values of the ground-state absorption cross section $\sigma_0(\lambda)$ were obtained from the UV−vis absorption spectrum; the singlet excited-state lifetime, from the decay of the femtosecond TA; the triplet excited state lifetime, from the decay of nanosecond TA; the triplet quantum yield, from the relative actinometry; and the effective triplet−triplet excited-state absorption cross section $\sigma_T(\lambda)$ was deduced from the femtosecond TA curve at 5.8 ns time delay in combination with the value of σ_T at 532 nm, 4.6×10^{-16} cm^2, which itself was determined from combined fitting of nanosecond and picosecond Z-scan data.[10] Detailed descriptions of the model and the fitting process have been reported by our group previously.[19]

Figure 5 shows representative Z scan experimental data and fitting curves for **1** at 532 and 760 nm at a series of different excitation energies. The resultant excited-state absorption cross sections and the two-photon absorption cross sections are displayed in Table 3. Figure 6 shows the time evolution of the population densities of the affected excited states during the course of a representative Z-scan pulse. We can see that below 600 nm, where the molecule has considerable ground-state absorption, both S_1 and S_2

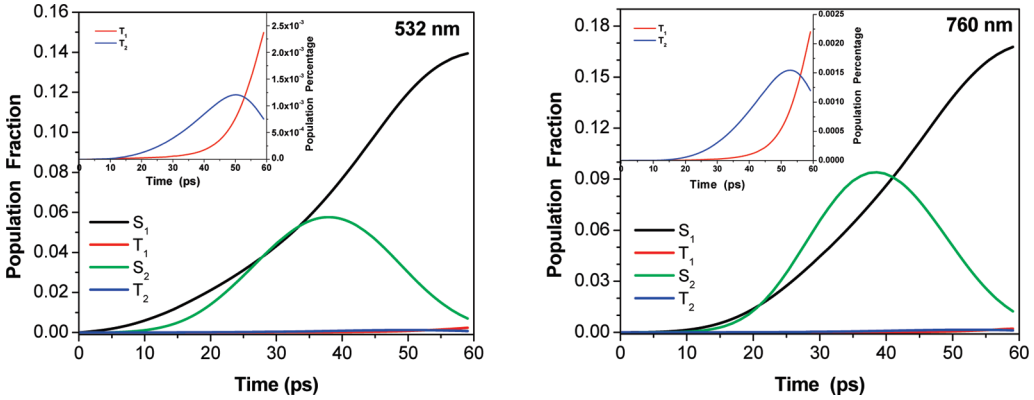

Figure 6. Fractional distribution of the populations of the affected excited states during a 21 ps laser pulse at 532 and 760 nm at the input face of the sample solution. The pulse energy used for the calculation is 3 μJ at 532 nm and 8 μJ at 760 nm.

have significant populations. We therefore take into account the contributions resulting from absorption from both S_1 and S_2 when fitting the Z scan data at these wavelengths. This gives rise to the cross sections shown in Table 3. At wavelengths greater than 600 nm, we were unable to detect measurable ground-state absorption even in a saturated solution of **1** over a 10 mm path length. For this reason, in the Z scans conducted at wavelengths of 630 nm and above, we assume that the excited states are populated by two-photon absorption. (Even so, it is quite possible that the rather high value, 1000 GM, of the two-photon absorption cross section σ_2 that is reported in Table 3 for 630 nm is inflated somewhat by a contribution from the unmeasurably small single-photon ground-state absorption. At even longer wavelengths, however, we expect this contribution to be completely negligible.) Thus, at wavelengths greater than 600 nm, the Z-scan signal manifests contributions not only from excited-state absorption but from two-photon absorption as well. In order to deconvolve these contributions in the Z scans at wavelengths of 630−825 nm and so obtain values for $\sigma_2(\lambda)$, we assume that the estimated values of $\sigma_S(\lambda)$ derived from the measured value $\sigma_S(532\text{ nm}) = 6 \times 10^{-17}$ cm^2 and the femtosecond transient difference absorption spectrum at zero time delay (listed in Table 3) are dominated by the absorption from S_1 alone and thus accurately reflect the singlet excited-state absorption seen in the Z scans. In point of fact, the σ_S values obtained from the femtosecond TA spectrum are actually effective cross sections that include contributions from both the absorption from S_1 and the absorption from S_2, though the relative importance of these contributions is unknown. In addition, the femtosecond TA data in the range 780−825 nm are themselves intrinsically somewhat problematic, due to incomplete filtering of the 800 nm fundamental laser beam from the TA signal. Above 825 nm, the TA could not be measured because of the detection limit of our spectrometer, leaving us with no basis on which to estimate the singlet and triplet excited-state absorption cross sections at the wavelengths of 825−900 nm. Consequently, the two-photon absorption cross sections given in Table 3 for the wavelengths 825−900 nm inclusive should be considered as effective cross sections for excited-state-assisted two-photon absorption.

The excited-state absorption cross sections shown in Table 3 are all in the range of 10^{-17} to 10^{-15} cm^2. These values are comparable to or even larger than those reported in the literature for other reverse saturable absorbers.[10,21a−21c,21e,25] Most importantly, because of the weak ground-state absorption of **1** in the visible to the near-IR region, the ratios of the excited-state absorption cross section to that of the ground state become extremely large when the wavelength becomes longer. To the best of our knowledge, these are the largest ratios reported to date for a reverse saturable absorbing molecule. In addition to these large ratios, the two-photon absorption cross sections at the near-IR region deduced for **1** are also the largest values reported for platinum complexes.[11,26] It is also worth noting that the TPA band maximum of **1** almost coincides with its corresponding one-photon absorption band maxima (Figure 7, noting that the σ_2 values at 630, 850, 875, and 900 nm are not counted in plotting because the σ_2 value at 630 nm possibly has some contribution from one-photon absorption and the σ_2 values at 850−900 nm are effective TPA cross sections with contributions from both TPA and excited-state

(25) (a) McKay, T. J.; Staromlynska, J.; Davy, J. R.; Bolger, J. A. *J. Opt. Soc. Am. B* **2001**, *18*, 358. (b) Guha, S.; Kang, K.; Porter, P.; Roach, J. E.; Remy, D. E.; Aranda, F. J.; Rao, D. V. G. L. N. *Opt. Lett.* **1992**, *17*, 264. (c) Perry, J. W.; Mansour, K.; Lee, I.-Y. S.; Wu, X.-L.; Bedworth, P. V.; Chen, C.-T.; Ng, D.; Marder, S. R.; Miles, P.; Wada, T.; Tian, M.; Sasabe, H. *Science* **1996**, *273*, 1533. (d) Song, Y.; Fang, G.; Wang, Y.; Liu, S.; Li, C. *Appl. Phys. Lett.* **1999**, *74*, 332. (e) Pittman, M.; Plaza, P.; Martin, M. M.; Meyer, Y. H. *Opt. Commun.* **1998**, *158*, 201. (f) Si, J.; Yang, M.; Wang, Y.; Zhang, L.; Li., C.; Wang, D.; Dong, S.; Sun, W. *Appl. Phys. Lett.* **1994**, *64*, 3083. (g) Sun, W.; Li, Y.; Pritchett, T. M.; Ji, Z.; Haley, J. E. *Nonlinear Opt., Quantum Opt.* **2010**, *40*, 163. (h) Li, Y.; Pritchett, T. M.; Shao, P.; Haley, J. E.; Zhu, H.; Sun, W. *J. Organomet. Chem.* **2009**, *694*, 3688. (i) Pritchett, T. M.; Sun, W.; Guo, F.; Zhang, B.; Ferry, M. J.; Rogers-Haley, J. E.; Shensky, W., III; Mott, A. G. *Opt. Lett.* **2008**, *33*, 1053. (j) Li, Y.; Pritchett, T. M.; Huang, J.; Ke, M.; Shao, P.; Sun, W. *J. Phys. Chem. A* **2008**, *112*, 7200. (k) Shao, P.; Li, Y.; Sun, W. *J. Phys. Chem. A* **2008**, *112*, 1172.

(26) (a) Chan, C. K. M.; Tao, C.-H.; Tam, H.-L.; Zhu, N.; Yam, V. W.-W.; Cheah, K.-W. *Inorg. Chem.* **2009**, *48*, 2855. (b) Glimsdal, E.; Carlsson, M.; Eliasson, B.; Minaev, B.; Lindgren, M. *J. Phys. Chem. A* **2007**, *111*, 244. (c) Westlund, R.; Glimsdal, E.; Lindgren, M.; Vestberg, R.; Hawker, C.; Lopez, C.; Malmström, E. *J. Mater. Chem.* **2008**, *18*, 166.

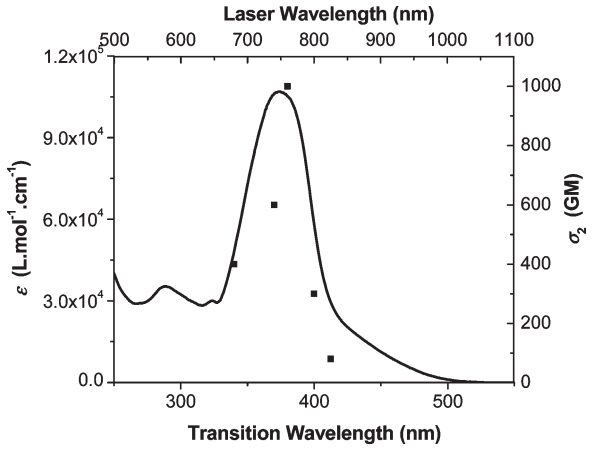

Figure 7. Two-photon absorption spectra (symbols) and one-photon absorption spectra (solid lines) of **1** in CH_2Cl_2.

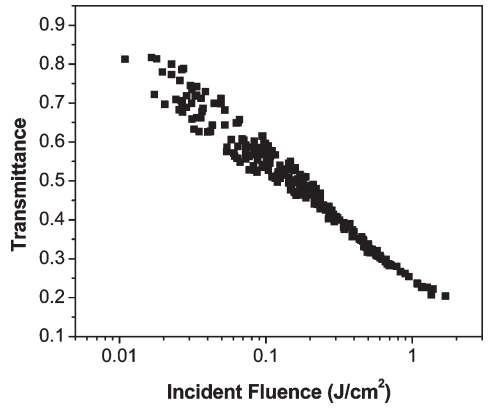

Figure 8. Transmission vs incident fluence curve for complex **1** in CH_2Cl_2 solution at 532 nm using 4.1 ns laser pulses. The linear transmission of the solution is 80% in a 2- mm cuvette. $c = 4.85 \times 10^{-3}$ mol/L.

absorption). Because of the lack of central symmetry of this complex and the approximate overlap of the TPA peak with its one-photon absorption peak, it is reasonable to conclude that the lowest-energy TPA transition of **1** corresponds to the $S_0 \rightarrow S_1$ transition.

Reverse Saturable Absorption. The Z scan experiments and fitting results discussed above imply that complex **1** could exhibit strong reverse saturable absorption in the visible spectral region due to the extremely large ratio of the excited-state absorption to that of the ground state. To demonstrate this, a nonlinear transmission experiment was carried out at 532 nm using 4.1 ns laser pulses. The result is shown in Figure 8. It is obvious that at the lowest detectable incident fluence (~0.01 J/cm^2), the transmission already deviates from the linear transmission, indicating that the threshold for reverse saturable is equal to or smaller than 0.01 J/cm^2. With increased fluence, the transmission keeps decreasing. At the incident fluence of ~1.6 J/cm^2, the transmission drops to 20%. This clearly manifests the reverse saturable absorption (RSA) at 532 nm. Referring to the population density shown in Figure 9 for nanosecond laser pulses at 532 nm, the observed RSA for the nanosecond laser pulse has contributions from both S_1 and T_1 absorption. The very large ratios of σ_{S1}/σ_0 and

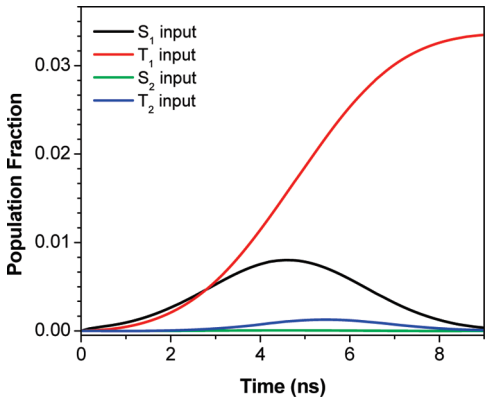

Figure 9. Fractional distribution of the populations of the affected excited states during a 4.1 ns laser pulse at 532 nm at the input face of the sample solution. The pulse energy used for the calculation is 5 μJ.

σ_T/σ_0 at 532 nm (shown in Table 3) lead to the strong reverse saturable absorption.

Conclusions

The platinum 2,2′-bipyridine complex bearing 2-(benzothiazol-2′-yl)-9,9-diethyl-7-ethynylfluorene ligands exhibits a strong absorption band at 374 nm in CH_2Cl_2 solution, which is attributed to the somewhat delocalized $^1\pi,\pi^*$ transition of the acetylide ligands. A broad, weak ^{1}MLCT band appears between 410 and 500 nm. It is emissive at room temperature and at 77 K. The emitting state at room temperature can be switched from the acetylide ligand localized $^3\pi,\pi^*$ state in polar solvents, such as CH_3CN and CH_2Cl_2, to the ^{3}MLCT state in less polar solvents such as hexane and toluene. The modulation of the order of the excited states by solvent polarity is supported by a transient absorption study using solvents of differing polarity. The most striking feature of complex **1** is its very broad and strong nonlinear absorption in the visible to the near-IR region, which manifests itself in extremely large ratios of the excited-state absorption cross section to that of the ground-state in the visible spectral region and in the largest two-photon absorption cross sections in the near-IR region compared to the other reported platinum complexes. This feature, along with its weak ground-state absorption in the visible to the near-IR region, makes complex **1** a very promising candidate for photonic devices that require large and broadband nonlinear absorption.

Acknowledgment. This work is supported by National Science Foundation (CAREER Grant CHE-0449598) and the Army Research Laboratory (Grant W911NF-06-2-0032).

Supporting Information Available: Normalized UV−vis absorption spectrum of **1** and **1-L** in different solvents, emission spectra of **1** in CH_2Cl_2 solution at different concentrations, and triplet transient difference absorption spectra of **1** in CH_3CN and in toluene (PDF). This material is available free of charge via the Internet at http://pubs.acs.org.